https://doi.org/10.36296/1819-8058.2025.4(83).126-135

PERFORMANCE ENHANCEMENT OF FLAT PLATE SOLAR PVT COLLECTOR USING ZN-ZNO/WATER HYBRID NANOFLUID

Received Aug. 05, 2025; accepted Dec. 09, 2025
Available online Dec. 31, 2025

Sakthivel K.[1], Dhanushkodi S.[2], Sudhakar K.[3], Balu P.[4], Ivanchuk V.[5]

Author for correspondence: Sakthivel K.
e-mail: ksmega6@gmail.com

[1] Research Scholar,
Department of Mechanical Engineering
https://orcid.org/0009-0006-5612-0070

[2] Professor,
Department of Mechanical Engineering
https://orcid.org/0000-0002-3473-872X

[3] Associate Professor,
Faculty of Mechanical Engineering
https://orcid.org/0000-0002-4867-2362

[4] Associate Professor
https://orcid.org/0000-0003-3480-1116

[5] PhD (Tech.), Research Assistant
https://orcid.org/0000-0002-0585-9610

[1, 2] PRIST University, Thanjavur, Tamil Nadu, India

[3] Malaysia University, Pahang, Malaysia

[4] Bharath Institute of Higher Education and Research, Chennai, Tamil Nadu, India

[5] Institute of Renewable Energy, NAS of Ukraine, Kyiv, Ukraine

Abstract. *Providing an analytical examination of the solar flat plate collector (SFPC) is the goal of this work. Using Zn/water, ZnO/water nanofluids, and Zn-ZnO/water hybrid nanofluid. This study compares various mass flow rates and concentrations of nanoparticles. Heat transfer, energy and exergy efficiency, and pressure drop characteristics of SFPC operation on these nanofluids are investigated. The addition of Zn/water nanofluid 16.71%, ZnO/water nanofluid 16.36%, and Zn-ZnO/water hybrid naofluid 18.52% nanoparticles enhances the working fluid's thermal conductivity. Gain in heat is improved with use of Nanofluids Zn/water nanofluid 1.02%, ZnO/water nanofluid 0.90%, Zn-ZnO/water hybrid nanofluid 2.15%. Efficiency improvements observed in SFPC Zn/water nanofluid: 0.93%, ZnO/water nanofluid 1.05%, Zn-ZnO/water hybrid nanofluid: 2.23%. The increase in pumping power required for the nanofluids: Zn/water nanofluid 3.08%, ZnO/water nanofluid 2.38%, Zn-ZnO/water hybrid nanofluid: 2.918%. Improvements in energy efficiency as per exergy analysis: Zn/water nanofluid 2.32%, ZnO/water nanofluid 2.18%, Zn-ZnO/water hybrid nanofluid 2.60%. In solar flat plate collectors, hybrid nanofluid Zn-ZnO/water significantly improves efficiency. The hybrid nanofluid exhibits the highest thermal conductivity and the most substantial improvement in collector efficiency and usable heat gain among the tested fluids. Additionally, despite a slight increase in pumping power requirements, the overall energy and exergy performance enhancements make hybrid nanofluids suitable for SFPC applications. These findings suggest that integrating hybrid nanofluids in SFPCs can lead to more efficient solar energy systems, potentially contributing to better energy management and sustainability. Further research could explore optimizing nanoparticle concentration and flow rates to maximize these benefits while managing pumping power requirements.*

Key words: *Solar flat plate collector, Thermo physical properties, Hybrid nanofluid, Energy efficiency, Exergy efficiency.*

ПІДВИЩЕННЯ ЕФЕКТИВНОСТІ ПЛОСКОГО СОНЯЧНОГО PVT-КОЛЕКТОРА ЗА РАХУНОК ВИКОРИСТАННЯ ГІБРИДНОГО НАНОРІДИННОГО ТЕПЛОНОСІЯ Zn–ZnO/ВОДА

Отримано 05 серп. 2025 р.; рекомендовано до публікації 09 груд. 2025 р.
Доступно онлайн 31 груд. 2024 р.

Сактивел К.[1], Дханушкоді С.[2], Судхакар К.[3], Балу П.[4], Іванчук В.[5]

Автор для кореспонденції: Сактивел К.,
e-mail: ksmega6@gmail.com

[1] аспірант кафедри машинобудування
https://orcid.org/0009-0006-5612-0070

[2] професор кафедри машинобудування
https://orcid.org/0000-0002-3473-872X

[3] доцент, факультет машинобудування
https://orcid.org/0000-0002-4867-2362

[4] доцент
https://orcid.org/0000-0003-3480-1116

[5] канд. тех. наук, науковий співроб.
https://orcid.org/0000-0002-0585-9610

Анотація. *Метою цієї роботи є аналіз робочих характеристик плоского сонячного колектора. Дослідження проводиться з використанням нанорідин Zn/вода, ZnO/вода та гібридної нанорідини Zn–ZnO/вода. У роботі порівняно різні витрати теплоносія та концентрації наночастинок. До-*

сліджено теплопередачу, енергетичну та ексергетичну ефективність, а також характер зміни гідравлічного опору при роботі плоского сонячного колектора з різними нанорідинами. Додавання нанорідини Zn/вода покращує теплопровідність робочої рідини на 16,71%, нанорідини ZnO/вода — на 16,36%, гібридної нанорідини Zn–ZnO/вода — на 18,52%. Приріст корисного тепла покращується за застосування нанорідини Zn/вода на 1,02%, ZnO/вода — на 0,90%, Zn–ZnO/вода — на 2,15%. Підвищення ефективності роботи плоского сонячного колектора становило у разі використання нанорідини Zn/вода 0,93%, ZnO/вода — 1,05%, Zn–ZnO/вода — 2,23%. Зростання потужності, необхідної на прокачування, складало у випадку застосування нанорідини Zn/вода 3,08%, ZnO/вода — 2,38%, Zn–ZnO/вода — 2,918%. Підвищення енергоефективності за результатами ексергетичного аналізу становило у випадку застосування нанорідини Zn/вода 2,32%, ZnO/вода — 2,18%, Zn–ZnO/вода — 2,60%. Гібридна нанорідина Zn–ZnO/вода демонструє значне підвищення ефективності плоского сонячного колектора, забезпечуючи найвищу теплопровідність та найбільший приріст енергоефективності серед досліджуваних робочих рідин у плоских сонячних колекторах.

Попри незначне збільшення енергоспоживання на прокачування, загальні показники енергетичної та ексергетичної ефективності свідчать про доцільність застосування гібридних нанорідин у колекторах такого типу. Отримані результати демонструють, що використання гібридних нанорідин підвищує ефективність сонячних систем генерації, покращує можливості енергоменеджменту та сприяє досягненню сталості. Подальші дослідження можуть бути спрямовані на оптимізацію концентрації наночастинок та витрат теплоносія в цілях максимізації ефекту та мінімізації витрат на перекачування.

[1, 2] Університет PRIST, Танджавур, Тамілнад, Індія

[3] Університет Малайзії, Паханг, Малайзія

[4] Інститут вищої освіти та досліджень Бхарат, Ченнаї, Тамілнад, Індія

[5] Інститут відновлюваної енергетики НАН України, Київ, Україна

Ключові слова: *інтеграція відновлюваної енергії, асинхронний двигун з подвійною кліткою (DCIM), енергоефективність, теплові характеристики, моментні характеристики, сталість транспорту, аналіз методом скінченних елементів (FEA), MATLAB-моделювання.*

1. INTRODUCTION

The spread of industrial development has led to an increase in the use of traditional fossil fuels. It is anticipated that by 2035 to 2040, the global share of renewable energy will rise by 14% to 22% [1]. Furthermore, within the past few decades, the use of solar energy has increased across a wide range of applications. Heat and electricity can be directly produced from solar energy. [2]. In order to accomplish this goal, thermal systems like photovoltaic thermal collectors, both evacuated tube collectors (ETC) and flat-plate solar collectors (FPSC) can be used. [3]. Solar energy is predominantly harnessed using solar thermal and photovoltaic technologies. With 8% of the installed capacity, solar photovoltaic technologies have primarily dominated the renewable energy market in India [4]. In a PV panel, a PV/T system produces electrical energy, while the cooling process uses a variety of materials and fluids, including air, water, the substance that changes phases and thermal energy absorption via nanofluids [5]. Nanoparticles enhance the outlet temperature of flat plate solar collectors [6]. Flat-plate collectors perform better than ETC in terms of exergy and energy efficiency when the gross area is equal [7]. PV/T systems with significant energy and performance gains can be constructed using the study's findings. [8]. Collector efficiency increases when TiO_2-water nanofluids are used instead of pure water [9]. Applying nanofluid is advised to boost the solar thermal/thermoelectric system's power output, carbon offset, and carbon credits [10]. The use of nanoparticles enhances their performance, and the micro-fin tube with twisted tape improves heat transfer, thereby enhancing thermal performance [11]. The nanofluid-cooled sinusoidal serpentine tube collector (PV/T-S) unit exhibits the optimum energetic and exergetic performance [12]. The findings show that, in comparison to pure water, the nanofluid enhances temperature performance and thermal efficiency [13]. When SiC nanofluid, TiO_2 nanofluid, SiO_2 nanofluid, and pure water were utilized as cooling fluids in the PV/T collector, the Pmax of the PV/T rose by 62.5%, 57%, 55%, and 50%, respectively. Additionally, it was found that the SiC/water nanofluid worked better electrically and thermally than other working fluids [14]. With the best overall energy coefficient (COE) of 0.93, the PV/T collector with SiC nanofluid has the maximum combined PV/T efficiency of 81.73% and PV/T electrical efficiency of 13.52% [15]. The sheet-and-sinusoidal tube collector (PV/TW) unit has total energy and energy efficiencies are 9.11 – 15.51% and 1.12 – 2.59% greater, respectively, compared to the PV/TP unit's sheet-and-plain tube collector [16]. The current study examined the stability of a distilled water/magnesium oxide (MgO) nanofluid and its effect on the FPSC thermal performance. Under the same parametric conditions, the absorbed energy factor rose by 16.74% while the heat loss parameter decreased by 52.2%. The outcomes support the application of MgO nanofluid in FPSC [17]. The ideal design for efficiently cooling photovoltaic panels is a PV module with bi-fluid modes, which can contribute to the development of more sustainable and energy-efficient solar energy conversion technologies [18]. The electrical energy efficiency increased when a hybrid nanofluid was used, and it was also used to cool the PV panels to achieve optimal performance [19]. The nanotubes give out the maximum thermo-hydraulic performance parameter [20]. Modern machine learning algorithms and hybrid nanofluids are being used to enhance FPSC's thermal performance. [21]. The performance of a Zn/ZnO hybrid nanofluid is tested. The current effort aims to investigate the performance of the SFPC using Zn-ZnO/water nanofluids. The trials were conducted at various flow rates and a fixed concentration inside an enclosed space. The outcomes are contrasted with SFPC based on water.

2. EXPERIMENT

2.1. Apparatus

The setup consists of a 30W mono-crystalline silicon photovoltaic module. The PV module specs are listed in Table 1, and Fig. 1 displays the schematic diagram. Thermal characteristics of the PVT panel material are given in Table 2. Copper tubes are arranged in a harp pattern at the base of the solar panel. The nanofluid is pumped through the cooling circuit. The nanofluid is heated in the PVT system and then cooled using a heat exchanger. The temperature of the nanofluid is measured using K-type thermocouples, and the surface temperatures of the solar modules are measured using temperature guns. Table 3 lists the electrical circuit specifications employed in the setup, whereas Table 4 lists the characteristics of the various nanomaterials.

A charge controller is connected with a switch between solar panels, batteries and consumer loads, enabling PVT systems to generate a sustained power source. The voltages and currents in open and short circuits are measured using digital multimeters, while hand-held solar power meters are used to detect solar radiation.

Table 1. Specifications of Photovoltaic Module

S.No.	Parameter	Specification
1.	Maximum Power (P_{max})	30 W
2.	Voltage in Open-circuit	22.0 V
3.	Current in Short-circuit	1.75 A
4.	Voltage at P_{max} (V_{mp})	18.5 V
5.	P_{max} Current (I_{mp})	1.62 A
6.	Efficiency	15%
7.	Type of PV module	Mono-crystalline silicon

Table 2. Thermal characteristics of PVT panel

S.No.	Description	Density (kilogram/cu.m)	Sp. Heat (J/kg·K)	Thermal Conductivity (W/m·K)
1	Glass	2,500	837	1.05
2	Silicon	2,330	700	148
3	Copper	8,960	385	401

Table 3. Specifications of Electrical Components

S.No.	Component	Specification
1	Charge Controller	10A PWM, 12V/24V
2	Storage Battery	100Ah Lead-acid, 12V,
3	Consumer DC Load	12V LED lights, 12V DC fan, USB charger

Table 4. Thermophysical characteristics of various base fluids and nanomaterials

S.No.	Cooling Fluid	Density (kg/ m3)	Sp.heat Capacity (J/kg-K)	Thermal Conductivity (W/m-K)
1	Water	997.1	4182	0.617
2	Zn	7130	523	50
3	ZnO	5600	501	16.1

3. SCHEMATIC ILLUSTRATION OF THE EXPERIMENTAL SETUP:

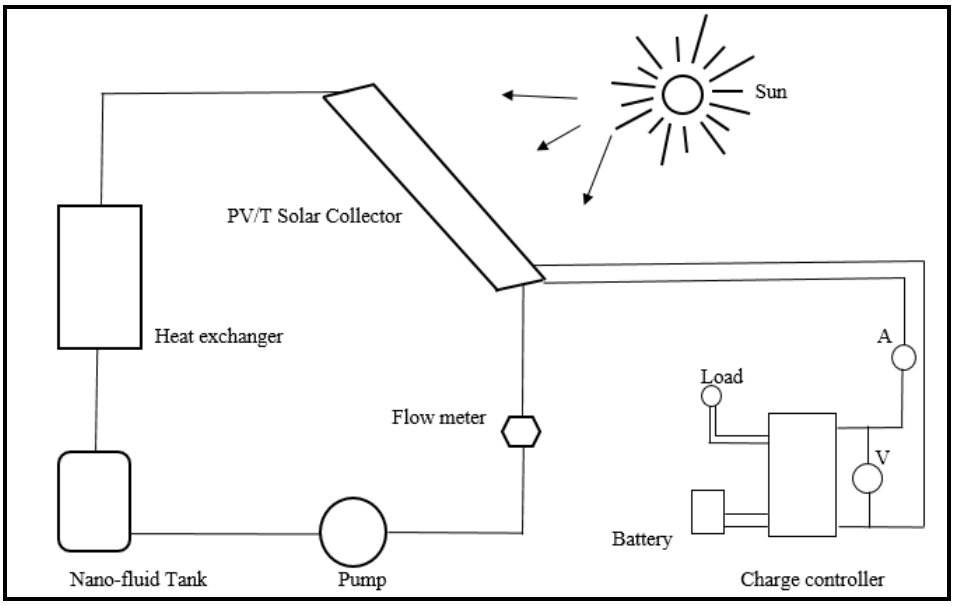

Fig. 1. Schematic diagram of the experimental setup

3.1. Composition of hybrid nanofluid

Fig. 2 displays the Zn, ZnO, and Zn-ZnO nanoparticles' scanning electron microscopy images, which Kanasparsa Chemicals Pvt. Ltd. supplies to produce Zn-ZnO hybrid nanofluid suspended in deionized water. The thermophysical characteristics of several base fluids and nanomaterials are listed in Table 4.

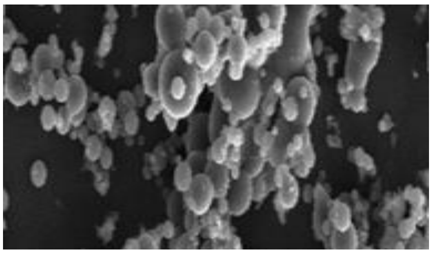

(a)

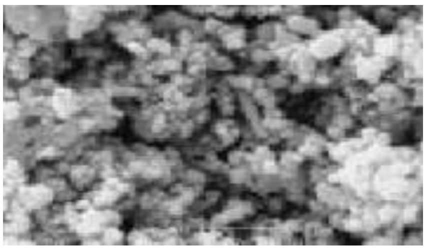

(b)

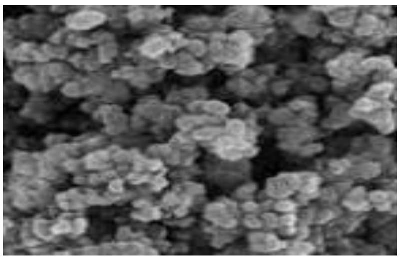

(c)

Fig. 2. SEM images of (a) Zn (b) ZnO and (c) Zn-ZnO hybrid nanoparticles

Both one-step and two-step procedures are commonly used to prepare nanofluids. SEM is referenced in Fig. 2. Nanoparticle images (a) of zinc nanoparticles (b) of zinc oxide nanoparticles (c) of zinc-zinc oxide hybrid nanoparticles. Zn, ZnO, and Zn-ZnO nanoparticles are suspended in deionized water to create a hybrid nanofluid.

3.2. Experimental procedure

1. **Setup initialization**:

- Ensure that all components are properly connected as per the schematic diagram in Fig. 1.
- Fill the cooling circuit with the selected nanofluid.
- Set the constant volume flow rate for the nanofluid pump.

2. **Measurement and data collection:**

- Using K-type thermocouples, note the nanofluid's initial temperature at the heat exchanger's input.
- The regular use of temperature guns to measure the solar panel's surface temperatures.
- Monitor and record the temperature of the nanofluid at various points in the cooling circuit.

3. **Cooling and efficiency evaluation:**

- Allow the system to run under stable solar radiation conditions.
- Measure the nanofluid's exit temperature after it has passed through the cooling system.
- Determine the heat transfer rate, cooling efficiency, and overall system efficiency using the recorded data.

4. **Data analysis:**

- Analyze the system's performance using various nanofluids.

- Analyze how the thermal characteristics of the nanofluid affect the PV/T system's overall efficiency.
- Evaluate the data to determine optimal nanofluid and flow rate for maximum efficiency and minimal temperature rise in the PV module.

The purpose of the experimental setup is to examine how various nanofluids affect the PV/T system's electrical and thermal performance, with a focus on optimizing the cooling process to enhance overall efficiency.

4. DATA REDUCTION AND MEASUREMENT

In this experiment, a 30W power hybrid PV/T module is used. PV panels are equipped with copper tubes at the back that are utilized to deliver hybrid nano-fluid at varying flow rates and fixed concentrations. An infrared thermometer is used to record the panel's temperature. Temperature measurements are obtained at the panel's entry and exit as well as the heat exchanger's entry and exit. Temperatures are recorded at several locations throughout the experimental setup using six thermocouples. The hot fluid is sent back to the panel's entry via a bucket after cooling in a finned heat exchanger. Solar radiation serves as the input energy,and the thermal and electrical energy are the outputs when the thermal collector and PV module are viewed as a single control volume.

Equation (1) gives Reynolds and Prandtl numbers

$$Re = \frac{4\, m_r}{\pi D_{i\mu}}$$

$$r = \frac{\mu C_p}{k} \quad (1)$$

where,

m_r - rate of mass flow in a single riser

Equation (2) gives Nusselt number of SFPC.

$$N_u = \frac{(f/8)(R_e-1000)P_r}{1+1.27\left(^f/_8\right)^{0.5}(P_r{}^{0.66}-1)} \quad (2)$$

Where,

f, - Darcy friction factor.

Equation (3) provides the working fluid's rate of useful heat gain based on the principles of thermodynamics.

$$Q_u = mC_p\,(T_{f,out}-T_{f,in}) \quad (3)$$

Equation (4) provides the working fluid's heat gain.

$$Q_u = A_c[I_t(r\alpha)-U_l(T_p-T_a)]$$

$$Q_u = [I_t(r\alpha)-U_l(T_{f,in}-T_a)] \quad (4)$$

Where,

F_R – heat removes factor

Equation (5) computes the pumping power.

$$P = \frac{m}{\rho_{nf}}\Delta p \quad (5)$$

Exergy efficiency is obtained by equation (6)

$$\eta_{Ex} = \frac{Ex_{gain}}{Ex_{sun}} = \frac{Ex_{out,f}-Ex_{in,f}}{I_t A_c\left(1-\frac{T_a}{T_{sun}}\right)} \quad (6)$$

In the SFPC, entropy is calculate by equation (7)

$$(S_{gen})H = \frac{Ex_{dest,1}+Ex_{dest,2}+Ex_{dest,3}+Ex_{leak}}{T_a}$$

$$(S_{gen})F = \frac{Ex_{dest\,\Delta p}}{T_a} \quad (7)$$

5. FINDINGS AND CONVERSATION

Effective thermal conductivity is the ratio of a nanofluid's thermal conductivity to that of the base fluid. As a function of particle concentration, Fig. 3 displays the effective thermal conductivity of the component mono and hybrid nanofluids.

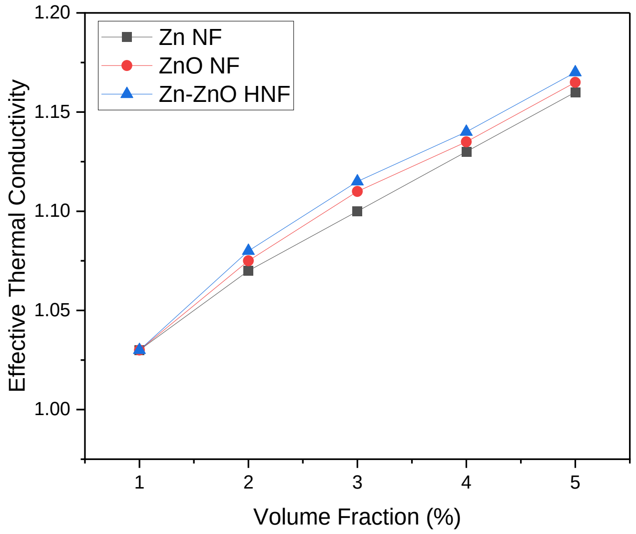

Fig. 3. Thermal Conductivity with respect to volume fraction

When compared to water, thermal conductivity is increased 16.71% for Zn/water, 16.36% for ZnO/water, and 18.52% for Zn-ZnO/water hybrid nanofluid. The effective thermal conductivity of mono- and hybrid-nanofluids is influenced by particle volume concentration; this effect is more pronounced at higher volume fractions. The reason for the enrichment is that the dynamic motion of the particles enhances collisions between suspended nanoparticles. This is the reason for the enrichment. When copper nanoparticles hybridize with copper oxide nanoparticles, Kim et al. claim that a superior thermal network is created at the particle-particle and particle-surrounded fluid layer interfaces [22].

The Nusselt number variation for mass flow rates of 0.1 kg/s and 0.5 kg/s is depicted in Figs. 4 (a) and (b). These are the Nusselt numbers: 78.28 and 12.54 at mass water flow rates of 0.1 kg/s and 0.5 kg/s, respectively. However, the Nusselt number of the nanofluid falls with increasing particle concentration, and the Reynolds number is inversely proportional to the fluid's viscosity at constant mass flow rates.

Thermal diffusion rates increase by 18.51% while viscous diffusion rates decrease by 4.4 % for Zn-ZnO/water hybrid nanofluid with a mass flow rate of 0.1 kg/s. As a result, the Nusselt number drops by 9.6%. At a mass flow rate of 0.5 kg/s, the Zn-ZnO/water hybrid nanofluid reduced the Nusselt number by 13.99% in comparison to water. This happens because, as the mass flow rate improves, the Reynolds number rises. Heat capacity falls, and the nanofluid's thermal conductivity rises more with larger particle density. Consequently, the Prandtl number lowers when thermal diffusion takes dominance over viscous diffusion. The decrease in Nusselt number is caused by the combined decline in Reynolds and Prandtl numbers.

The Nusselt number fluctuation as a function of Reynolds number is displayed in Fig. 5 for a variety of nanofluids with different particle concentrations ranging from 1 vol.% to 5 vol.%. In SFPC, the mass flow rate rises proportionately to the nanofluid's Reynolds number. Regardless of the kind of nanofluid, the Nusselt number increases as the Reynolds number does. According to Allahyar et al., the Nusselt number increases as the Reynolds number does [23]. The change in outlet temperature in relation to volume fractions at mass flow rates of 0.01 kg/s and 0.1 kg/s is depicted in Figs. 6 (a) and (b). The working fluid's specific heat significantly affects the nanofluid's exit temperature in an SFPC. Zinc/water has a lower heat capacity and higher density than other nanofluids, resulting in higher outlet temperatures.

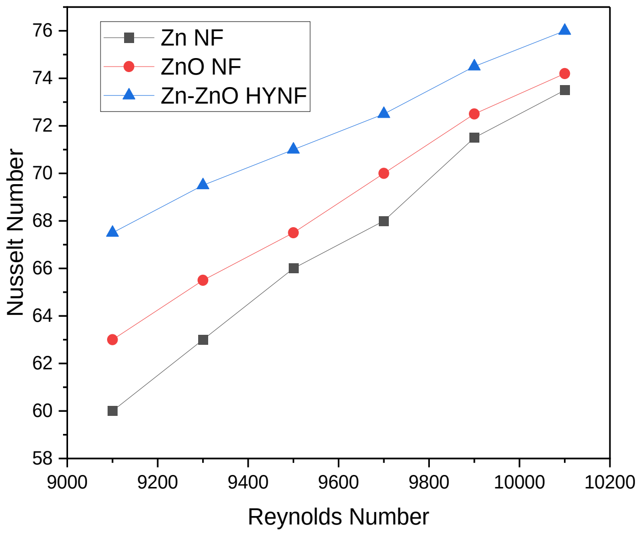

Fig. 5. Reynolds number in relation to Nusselt number

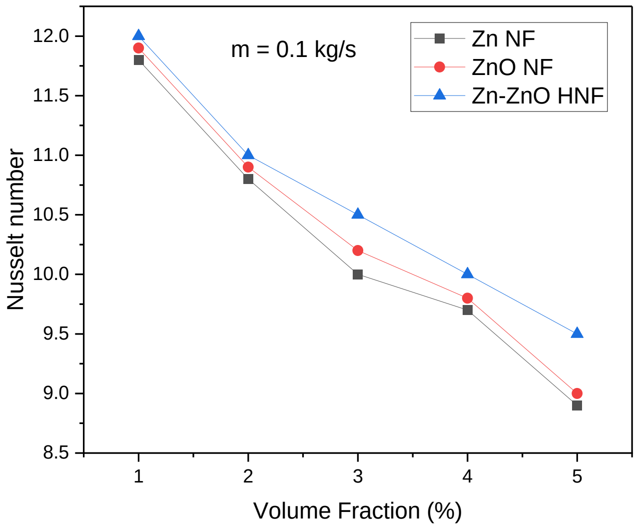

Fig. 4 (a). Nusselt number with respect to the particle volume fraction

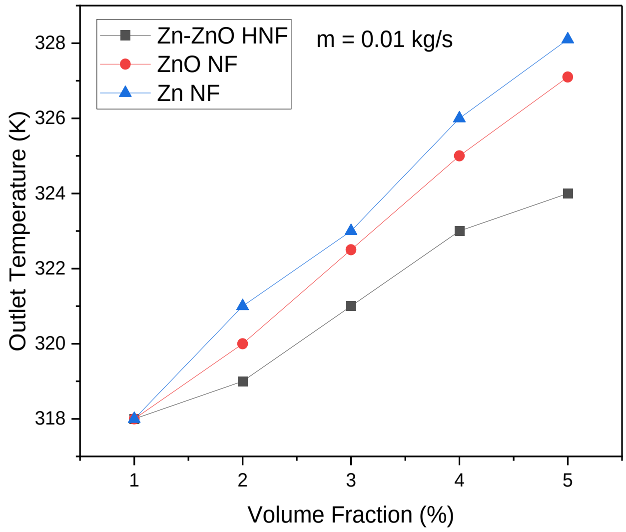

Fig. 6 (a). Temperature at the outlet in relation to the particle volume faction

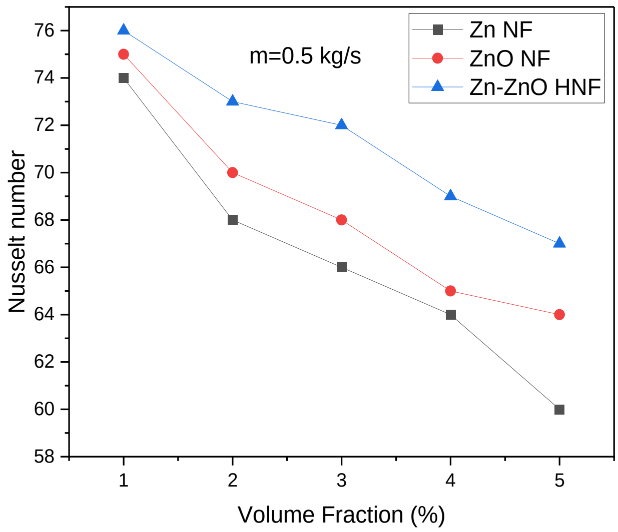

Fig. 4 (b). Nusselt number in relation to the fraction of particle volume

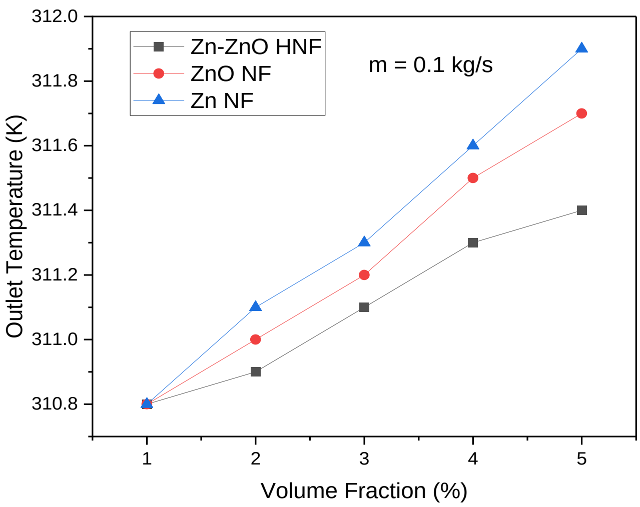

Fig. 6 (b). Temperature at the outlet in relation to the particle volume fraction

The outlet temperature is not solely determined by specific heat. Because the higher effective density nanofluid has a lower velocity at a given flow rate, it may absorb more heat energy from the hot riser tube of the SFPC. As a result, the nanofluid's exit temperature rises. According to Genc et al., the nanoparticles have a stronger impact on the outlet temperature of the flat plate solar collectors [24]. Figs. 7 (a) and (b) display the heat gain at different volume percentages. These graphs demonstrate that the hybrid nanofluid has a higher heat gain than the mono nanofluids for all volume fractions. At a mass flow rate of 0.1 kg/s, the highest useful heat gain of the hybrid nanofluid is around 585.85 W/m_2, which is higher than the maximum usable heat gains of water, Zn/water, and ZnO/water nanofluids, which are 569.23 W/m^2, 574.23 W/m^2, and 575.11 W/m^2.

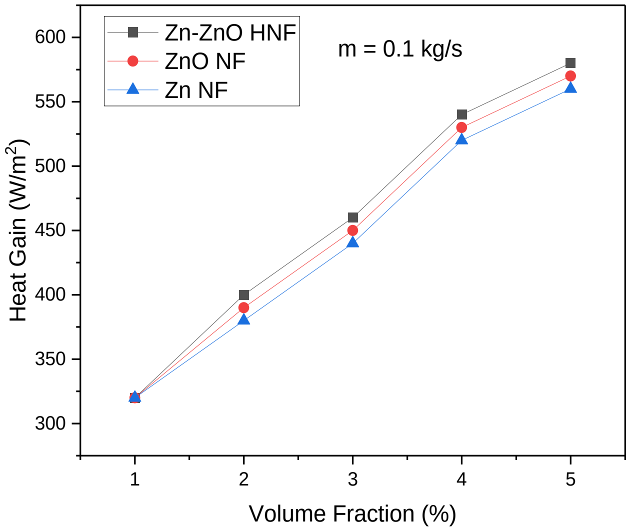

Fig. 7 (a). Heat gain with respect to particle volume fraction

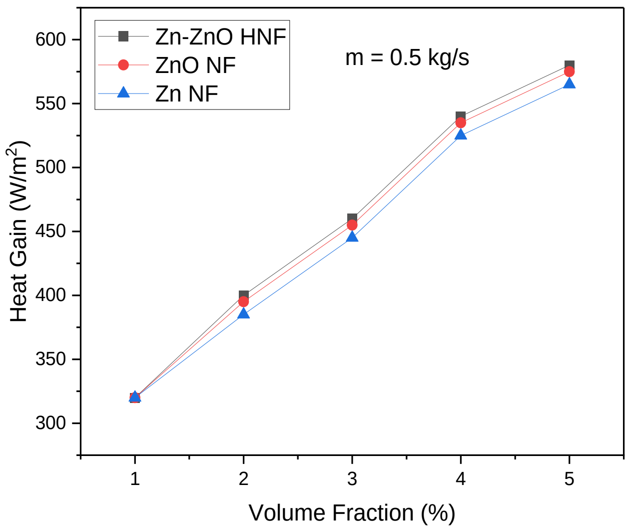

Fig. 7 (b). Heat gain in relation to the volume proportion of particles

The hybrid nanofluid has a heat gain of 601.41 W/m^2 at a mass flow rate of 0.5 kg/s. The equivalent gains for Zn/water, ZnO/water, and water nanofluids are 588.68 W/m^2, 591.14 W/m^2, and 593.23 W/m^2, respectively. The maximal usable heat gain of the hybrid nanofluid is precisely 2.15% more than that of water. The hybrid nanofluid's increased specific heat causes it to absorb more heat than the other nanofluids. According to Alrowaili and associates, the heat removal was 0.894. With a thermal-optical efficiency that is 61.7% higher than that of water and 14.9% higher than that of mono CuO, the hybrid CuO 2.5g and Cu 1.5g nanofluid [25]. Figs. 8 (a), (b) shows the SFPC's first law efficiency at various volume fractions of particle concentration in the Zn-ZnO/water hybrid nanofluid and its component mono nanofluids at mass flow rates of 0.1 kg/s and 0.5 kg/s. The hybrid nanofluid-based SFPC shows a 2.23% gain in instantaneous efficiency over water at a mass flow rate of 0.5 kg/s. The figure illustrates the superior performance of hybrid nanofluids over regular nanofluids in terms of collector efficiency at both mass flow rates.

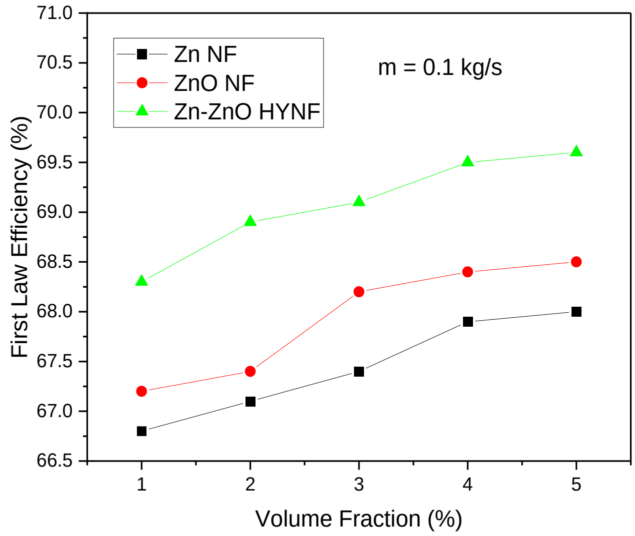

Fig. 8 (a). Thermal efficiency with respect to particle volume fraction

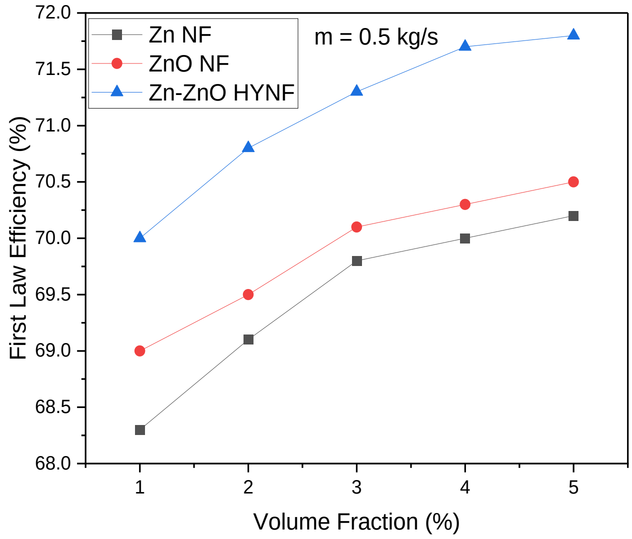

Fig. 8 (b). Thermal efficiency with respect to particle volume fraction

Higher energy efficiency is achieved by the collector fluid with a higher useful heat gain and a lower heat loss for the incident solar radiation. According to Zadkhast et al., the hybrid nanofluid's thermal conductivity significantly increases as the temperature and solid volume fraction rise [26]. For different nanofluids, the variation in SFPC's pumping power and pressure drop as a function of volume percent is shown. in Figs. 9 (a) and (b). When the volume fraction rises, the pressure drop increases linearly. Every nanofluid has a similar propensity to develop. As pressure decreases, the pumping power varies significantly. A greater pumping power is needed in proportion to the increased pressure loss in the Zn/water nanofluid. In contrast with water, the ZnO/water, Zn-ZnO/water, and Zn/water nanofluids exhibit gains in pumping power of 2.918%, 3.08%, and 2.38%, respectively.

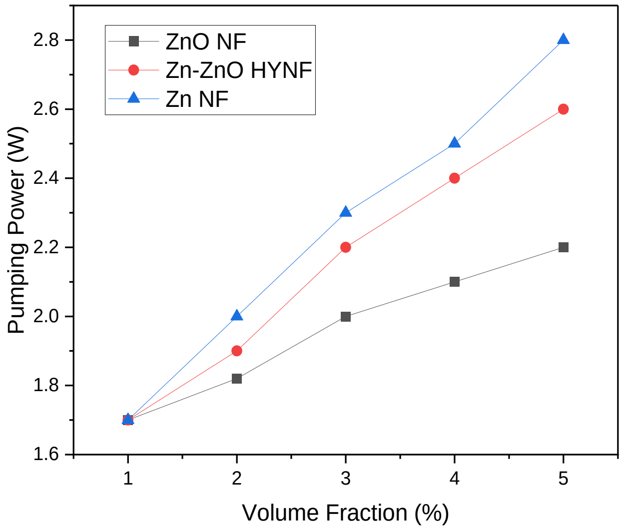

Fig. 9 (a). Pumping power with respect to particle volume fraction

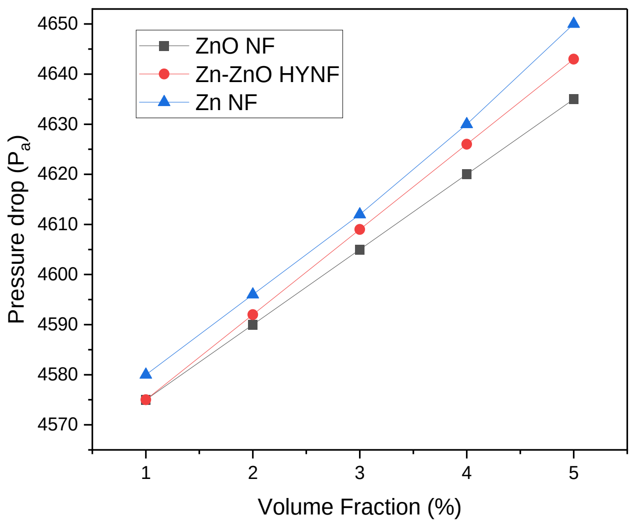

Fig. 9 (b). Drop in pressure relative to the particle volume fraction

Due to its maximum density, the Zn/water nanofluid produces a larger pressure drop than the other nanofluids. Moreover, viscosity is another element influencing pressure drop. Ajeena et al. reported that a ZrO_2-SiC/DW hybrid nanofluid required more pumping power than water and that a higher concentration of nanoparticles in the fluid resulted in a greater pressure drop [27]. Figs. 10 (a) and (b) show the second law efficiency of SFPC as a function of particle concentration for a variety of nanofluids at mass flow rates of 0.5 kg/s and 0.1 kg/s. Exergy efficiency is defined as the ratio of the net exergy obtained by the working fluid to the available exergy of the collector. The specific heat of the hybrid nanofluid is 4.49 % lower than that of the base fluid. Its efficiency of energy increases by 2.60 %. Mouli et al. discovered that the exergy efficiency increases as the volume percentage of nanoparticles increases [28].

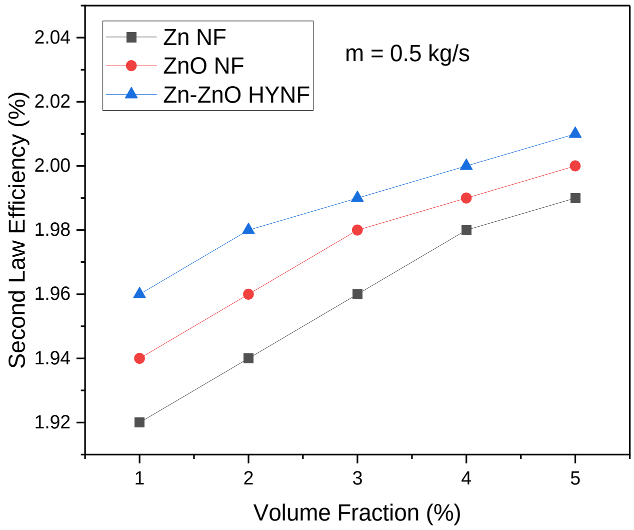

Fig. 10 (a). Exergy efficiency with respect to particle volume fraction

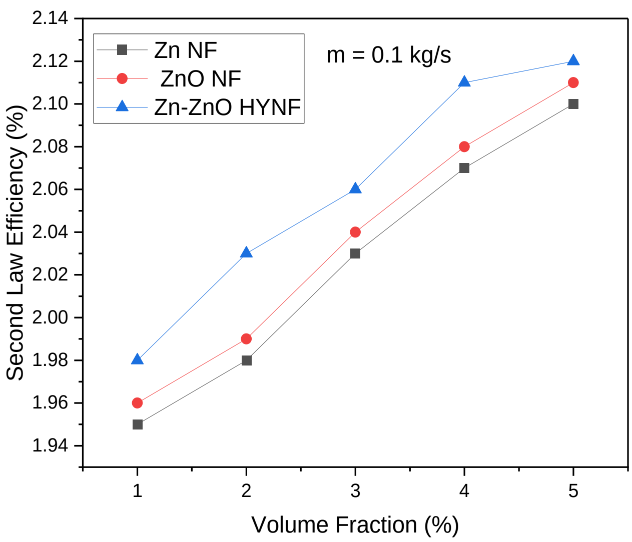

Fig. 10 (b). Exergy efficiency with respect to particle volume fraction

6. CONCLUSIONS

Metallic nanoparticles possess superior thermal transport characteristics and are intrinsically highly reactive. Hybrid nanofluids were developed to maximize the synergistic effects of suspensions containing monometallic nanoparticles. Consequently, hybridizing nanoparticles with metal oxides results in enhanced thermophysical properties. These improved thermophysical characteristics in solar flat plate collectors (SFPCs) lead to higher energy and exergy efficiencies. In this study, hybrid nanofluid Zn–ZnO/water and its constituent mono nanofluids were used to evaluate the first and second law performance of SFPCs, and the results were compared with those obtained using water.

1. **Energy and Exergy Efficiency:** Exergy data showed that the hybrid nanofluid increased energy efficiency by 2.60%. On the other hand, the exergy efficiency of the Zn/water and ZnO/water nanofluids increased by 2.18 and 2.32%, respectively.
2. **Useful Heat Gain**: The usable heat gain of ZnO/water, hybrid nanofluid, and Zn/water nanofluids increased by 1.02%, 2.15%, and 0.90%, respectively, due to the improvement in thermophysical characteristics.
3. **Thermal Conductivity**: While the Zn/water and ZnO/water nanofluids demonstrated improvements of 16.71% and 16.36%, respectively, the Zn-ZnO/water hybrid nanofluid demonstrated a gain of 18.52% in thermal conductivity when compared to water.
4. **Collector Efficiency**: The hybrid nanofluid's collector efficiency rose by 2.23%. 1.05% for the ZnO/water nanofluid, and 0.93% for the Zn/water nanofluid when compared to water.
5. **Pressure Drop**: The Zn-ZnO/water, ZnO/water and Zn/water nanofluids exhibit a penalty in terms of pressure drop, with increases of 2.918%, 2.38%, and 3.08%, respectively, in comparison to water.

Zn-ZnO/water hybrid nanofluid significantly enhances the performance of SFPCs, providing notable improvements in thermal conductivity, useful heat gain, and energy efficiency, despite the associated increase in pressure drop.

REFERENCES

1. Pang, W., Cui, Y., Zhang, Q., Wilson, Gregory. J., & Yan, H. (2020). A comparative analysis on performances of flat plate photovoltaic/thermal collectors in view of operating media, structural designs, and climate conditions. Renewable and Sustainable Energy Reviews, 119, 109599. https://doi.org/10.1016/j.rser.2019.109599
2. Moosavi, R., & Ahmadinejad, M. (2022). Energy and exergy evaluation of a baffled-nanofluid-based Photovoltaic Thermal System (Pvt). SSRN Electronic Journal. https://doi.org/10.2139/ssrn.4255389
3. Huminic, G., & Huminic, A. (2024). Capabilities of advanced heat transfer fluids on the performance of Flat Plate Solar Collector. Energy Reports, 11, 1945–1958. https://doi.org/10.1016/j.egyr.2024.01.044
4. Chandan, Suresh, V., Iqbal, S. Md., Reddy, K. S., &Pesala, B. (2021). 3-D Numerical Modelling and experimental investigation of coupled photovoltaic thermal and flat plate collector. Solar Energy, 224, 195–209. https://doi.org/10.1016/j.solener.2021.05.079
5. Ould-Lahoucine, C., Ramdani, H., &Zied, D. (2021). Energy and exergy performances of a TiO2-water nanofluid-based hybrid photovoltaic/thermal collector and a proposed new method to determine the optimal height of the rectangular cooling channel. Solar Energy, 221, 292–306. https://doi.org/10.1016/j.solener.2021.04.027
6. Genc, A. M., Ezan, M. A., &Turgut, A. (2018). Thermal performance of a nanofluid-based flat plate solar collector: A transient numerical study. Applied Thermal Engineering, 130, 395–407. https://doi.org/10.1016/j.ap plthermaleng.2017.10.166
7. Eltaweel, M., Abdel-Rehim, A. A., &Attia, A. A. A. (2021). A comparison between flat-plate and evacuated tube solar collectors in terms of energy and exergy analysis by using nanofluid. Applied Thermal Engineering, 186, 116516. https://doi.org/10.1016/j.applthermaleng.2020.116516
8. Shahsavar, A., Jha, P., Arıcı, M., Nižetić, S., & Ma, Z. (2021). Energetic and exergetic performances of a nanofluid-based photovoltaic/thermal system equipped with a sheet-and-grooved serpentine tube collector: Indoor Experimental Tests. Solar Energy, 225, 918–933. https://doi.org/10.1016/j.solener.2021.08.005
9. Moravej, M., Bozorg, M. V., Guan, Y., Li, L. K. B., Doranehgard, M. H., Hong, K., &Xiong, Q. (2020). Enhancing the efficiency of a symmetric flat-plate solar collector via the use of rutile TiO2-water nanofluids. Sustainable Energy Technologies and Assessments, 40, 100783. https://doi.org/10.1016/j.seta.2020.100783
10. Soltani, S., Kasaeian, A., Lavajoo, A., Loni, R., Najafi, G., & Mahian, O. (2020). Exergetic and Environmental Assessment of a photovoltaic thermal-thermoelectric system using nanofluids: Indoor Experimental Tests. Energy Conversion and Management, 218, 112907. https://doi.org/10.1016/j.enconman.2020.112907
11. Bassam, A. M., Sopian, K., Ibrahim, A., Al-Aasam, A. B., &Dayer, M. (2023). Experimental Analysis of Photovoltaic Thermal Collector (Pvt) with Nano PCM and micro-fins tube counterclockwise twisted tape nanofluid. Case Studies in Thermal Engineering, 45, 102883. https://doi.org/10.1016/j.csite.2023.102883
12. Shahsavar, A. (2021). Experimental Evaluation of Energy and exergy performance of a nanofluid-based photovoltaic/thermal system equipped with a sheet-and-sinusoidal serpentine tube collector. Journal of Cleaner Production, 287, 125064. https://doi.org/10.1016/j.jcle pro.2020.125064
13. Noghrehabadi, A., Hajidavalloo, E., & Moravej, M. (2016). Experimental investigation of efficiency of square flat-plate solar collector using SiO2 /water nanofluid. Case Studies in Thermal Engineering, 8, 378–386. https://doi.org/10.1016/j.csite.2016.08.006
14. Hasan, H. A., Sopian, K., Jaaz, A. H., & Al-Shamani, A. N. (2017). Experimental investigation of jet array nanofluids impingement in photovoltaic/thermal collector. Solar Energy, 144, 321–334. https://doi.org/10.1016/j.solener.2017.01.036
15. Al-Shamani, A. N., Sopian, K., Mat, S., Hasan, H. A., Abed, A. M., & Ruslan, M. H. (2016). Experimental studies of rectangular tube absorber photovoltaic thermal collector with various types of nanofluids under the tropical climate conditions. Energy Conversion and Management, 124, 528–542. https://doi.org/10.1016/j.encon man.2016.07.052
16. Varmira, K., Baseri, M. M., Khanmohammadi, S., Hamelian, M., & Shahsavar, A. (2021). Experimental study of the effect of sheet-and-sinusoidal tube collector on the energetic and exergetic performance of a photovoltaic-thermal

unit filled with biologically synthesized water/glycerol-silver nanofluid. Applied Thermal Engineering, 186, 116518. https://doi.org/10.1016/j.applthermaleng.2020.116518

17. Choudhary, S., Sachdeva, A., & Kumar, P. (2020). Investigation of the stability of MgOnanofluid and its effect on the thermal performance of Flat Plate Solar Collector. Renewable Energy, 147, 1801–1814. https://doi.org/10.1016/j.renene.2019.09.126
18. Khelifa, A., Kabeel, A. E., Attia, M. E., Abdelgaied, M., Arıcı, M., & Abdel-Aziz, M. M. (2023). 3D numerical analysis of a photovoltaic thermal using bi-fluid: Al2O3–water nanofluid at various concentrations. International Journal of Thermofluids, 20, 100523. https://doi.org/10.1016/j.ijft.2023.100523
19. Murtadha, T. K. (2023). Effect of using Al2O3 / TiO2 hybrid nanofluids on improving the photovoltaic performance. Case Studies in Thermal Engineering, 47, 103112. https://doi.org/10.1016/j.csite.2023.103112
20. Nuhash, M. M., Alam, M. I., Zihad, A., Hasan, M. J., Duan, F., Bhuiyan, A. A., & Karim, M. R. (2023). Enhancing energy harvesting performance of a flat plate solar collector through integrated carbon-based and metal-based nanofluids. Results in Engineering, 19, 101276. https://doi.org/10.1016/j.rineng.2023.101276
21. Said, Z., Sharma, P., Sundar, L. S., Li, C., Tran, D. C., Khoa Pham, N. D., & Nguyen, X. P. (2022). Improving the thermal efficiency of a solar flat plate collector using MWCNT-Fe3O4/water hybrid nanofluids and ensemble machine learning. Case Studies in Thermal Engineering, 40, 102448. https://doi.org/10.1016/j.csite.2022.102448
22. Kim, D., Kwon, Y., Cho, Y., Li, C., Cheong, S., Hwang, Y., Lee, J., Hong, D., & Moon, S. (2009a). Convective heat transfer characteristics of nanofluids under laminar and turbulent flow conditions. Current Applied Physics, 9(2). https://doi.org/10.1016/j.cap.2008.12.047
23. Allahyar, H. R., Hormozi, F., & ZareNezhad, B. (2016a). Experimental investigation on the thermal performance of a coiled heat exchanger using a new hybrid nanofluid. Experimental Thermal and Fluid Science, 76, 324–329. https://doi.org/10.1016/j.expthermflusci.2016.03.027.
24. Genc, A. M., Ezan, M. A., & Turgut, A. (2018). Thermal performance of a nanofluid-based flat plate solar collector: A transient numerical study. Applied Thermal Engineering, 130, 395–407. https://doi.org/10.1016/j.ap plthermaleng.2017.10.166
25. Alrowaili, Z. A., Ezzeldien, M., Shaaalan, N. M., Hussein, E., & Sharafeldin, M. A. (2022). Investigation of the effect of hybrid Cuo-cu/water nanofluid on the solar thermal energy storage system. Journal of Energy Storage, 50, 104675. https://doi.org/10.1016/j.est.2022.104675
26. Zadkhast, M., Toghraie, D., & Karimipour, A. (2017). Developing a new correlation to estimate the thermal conductivity of MWCNT-cuo/water hybrid nanofluid via an experimental investigation. Journal of Thermal Analysis and Calorimetry, 129(2), 859–867. https://doi.org/10.1007/s10973-017-6213-8.
27. Ajeena, A. M., Farkas, I., & Víg, P. (2023). Performance enhancement of flat plate solar collector using ZRO2-SiC/DW Hybrid Nanofluid: A comprehensive experimental study. Energy Conversion and Management: X, 20, 100458. https://doi.org/10.1016/j.ecmx.2023.100458
28. Mouli, K. V. V., Sundar, L. S., Alklaibi, A. M., Said, Z., Sharma, K. V., Punnaiah, V., & Sousa, A. C. M. (2023). Exergy efficiency and entropy analysis of MWCNT/water nanofluid in a thermosyphon flat plate collector. Sustainable Energy Technologies and Assessments, 55, 102911. https://doi.org/10.1016/j.seta.2022.102911